Hindawi
Geofluids
Volume 2022, Article ID 2831263, 11 pages
https://doi.org/10.1155/2022/2831263

Research Article

Variations of the Physical and Mechanical Parameters of Oil Sand under Different Confining Pressure and Temperatures

Liu Yang[1,2] **Yufei Jiang**[1] **and Chao Gao**[2]

[1]*Department of Civil Engineering, Sichuan University Jinjiang College, Meishan 620860, China*
[2]*Sichuan Commercial Investment Group Co. LTD., Chengdu 610041, China*

Correspondence should be addressed to Liu Yang; liu.yang929@hotmail.com and Yufei Jiang; 903919596@qq.com

Received 30 November 2021; Accepted 31 December 2021; Published 29 January 2022

Academic Editor: Yanan Gao

Oil sand is an important substitute for conventional oil resources. In this paper, oil sand cores are used to systematically study the mesostructure characteristics of oil sand. Triaxial compression tests under different temperatures and pressures are carried out on oil sand specimens. The research results show that the mineral particles in these oil sands have a loose structure. The particle size distribution of the mineral particles has good continuity. The prepeak deformation characteristics of these oil sands are similar. However, three kinds of postpeak deformation forms are observed: plastic flow, strain softening, and strain hardening. Increasing the temperature can enhance the shear dilatation rate, and the shear dilatation rate decreases nonlinearly with increasing confinement. The compressive strength, residual strength, and elastic modulus increase linearly with increasing confinement. Temperature has little effect on the strength and elastic modulus of oil sand, but it can significantly affect the corresponding Poisson's ratio. The failure modes of oil sand are dominated by shear failure and tensile failure. Under the test condition of 120°C, the thermal stress generated by the high temperature causes the oil sand specimens to produce transverse cracks. These results can provide relevant parameters for the design of oil sand exploration technology.

1. Introduction

Oil sand hosts heavy oil and asphalt and other unconventional oil and gas resources [1, 2]. Oil sands have considerable exploitation potential and can supplement for conventional oil resources and other chemical products [3, 4]. At present, the exploitation technologies of oil sand mainly include hydrothermal cracking, underground catalytic transformation, steam-assisted gravity drainage, enhanced circulation steam extraction, sand production, and cold exploitation. Among them, the main technology that can be applied is steam-assisted gravity drainage [5, 6] in which high-temperature steam is injected into oil sand reservoirs for reservoir stimulation to improve the flow properties of heavy oil and enhance reservoir permeability [7]. In the oil sand exploitation at Fengcheng Oilfield, steam-assisted gravity drainage technology is adopted. The practice shows that microfracturing with injected steam can effectively improve the permeability and enhance the oil sand recovery [8, 9]. The physical and mechanical properties of oil sand under in situ reservoir conditions (different geostresses and temperatures) directly affect the technical parameters and the hydraulic fracturing design [10–12]. Therefore, it is necessary to systematically study the physical and mechanical properties of oil sand at different temperatures and confining pressures.

Canada has the largest amount of oil sand reserves of any country worldwide, with the characteristics of deep burial depth, easy exploitation, and high oil content [13]. Dusseault and Morgenstern [14] carried out conventional triaxial compression experiments of Athabasca oil sand at room temperature to study the shear properties of oil sand, indicating that oil sands have almost no cohesion and that the self-locking among the mineral particles in oil sand was the main source of shear strength. Aiban [15] studied the effect of temperature on the shear properties of Athabasca oil sand, finding that high temperatures have little effect on the shear strength of oil sand but have a great effect on the pore pressure, and considered that a hyperbolic model can fit the deformation curve of oil sand well. Wong

et al. [16] systematically studied the variation characteristics of stress-strain curves of Cold Lake oil sand under triaxial compression with different loading paths and found that the stress-strain curves of oil sand under different confining pressures exhibit four different modes: shear swelling under strain softening, shear swelling under strain hardening, volume compression under strain hardening, and mineral particle crushing under strain hardening. Samieh and Wong [17] analyzed the influence of boundary conditions on the mechanical properties of oil sand in a triaxial compression experiment and found that the slenderness ratio and surface roughness of a cylindrical oil sand specimen have a great influence on its initial elastic modulus, dilatation rate, and postpeak softening rate. Ardeshir and Tim [18] tested the deformation characteristics of oil sand under periodic loading to determine an empirical formula of deformation with load. Wang and Wong [19] studied the creep characteristics of oil sand under triaxial compression and considered that the creep deformation of oil sand depends on the development of the external deflection stress, initial inelastic strain, and shear zone and proposed an oil sand creep model.

With the successful exploitation of oil sand resources in the Xinjiang Fengcheng Oilfield, its physical and mechanical properties have also attracted attention. Wang et al. [20] analyzed the creep characteristics of oil sand under different deviatoric stresses, proposed the creep and plastic potential to describe the creep and plastic deformation of oil sand, and established an internal variable model of oil sand creep. Qiao et al. [21] analyzed the properties of Fengcheng oil sand by X-ray diffraction, CT scanning, and triaxial compression experiments at room temperature and found that the properties of Fengcheng oil sand are similar to those of medium dense sand; additionally, the shear shrinkage or shear expansion properties were observed in the process of triaxial compression. Li et al. [22] carried out conventional triaxial compression experiments on Fengcheng oil sand at different temperatures and analyzed the variation in mechanical parameters such as the elastic modulus, Poisson's ratio, internal friction angle, cohesion, and thermal expansion coefficient at different temperatures and confining pressures. Wang et al. [23] analyzed the constitutive characteristics of Fengcheng oil sand and concluded that in soil mechanics, the Nanshui model and Chengdu University of Science and Technology model can fit the stress-strain relationship of oil sand well. Gao et al. [24] systematically summarized the effects of temperature on the mechanical properties of oil sand and found that when the temperature increases from 20°C to 250°C, the mechanical parameters of oil sand can change 0.25~3 times, indicating that the mechanical parameters of oil sand are sensitive to temperature, and three models of the evolution of oil sand mechanical parameters with temperature were proposed. Lin et al. [25] studied the shear mechanism of oil sand experimentally. Compared with Alberta oil sand in Canada, Fengcheng oil sand has a low consolidation degree and relatively loose structure, which leads to a smaller shear angle. Therefore, the technical parameters of Fengcheng oil sand exploitation will be different from those of Alberta oil sand exploitation. Pang et al. [26] analyzed the variation law of elastic mechanical parameters of oil sand under the influence of temperature by means of the Eshelby method, Mori–Tanaka method, and differential method to guide oil sand exploitation. The physical and mechanical properties of oil sand are of great significance to the design of oil sand exploitation technical schemes.

In this paper, taking oil sand reservoir core from the Xinjiang Fengcheng Oilfield at a depth of more than 400 meters as the research object, the mesoscopic structure of the oil sand was systematically tested, and conventional triaxial compression experiments under different temperatures and confining pressures were carried out. Then, the mineral composition, cementation state, and particle size distribution characteristics of Fengcheng oil sand were studied, and the variations in the oil sand mechanical parameters under different temperatures and pressures were analyzed. The failure mode of oil sand under different experimental conditions was also carefully discussed in detail to provide reliable physical and mechanical parameters for the design of oil sand exploitation technology in the Fengcheng Oilfield.

2. Research Methods

2.1. Preparation of Oil Sand Specimens. The oil sand is obtained from underground reservoir by coring. The diameter of the core was 110 mm, which was easily disturbed at room temperature, so the oil sand core was immediately placed in a refrigerator at -18°C after coring (Figure 1). The complete and intact oil sand core was processed into a cylinder with a height of 200 mm and a diameter of 100 mm under freezing conditions by lathe. The allowable deviation of the diameter of the specimen was less than 2 mm, the allowable deviation of the height was less than 4 mm, the allowable deviation of the flatness of the two ends was less than 0.5 mm, and the vertical deviation from the axis was within ±1°. The geometric size of the specimen met the requirements of the rock mechanical experiment. The rock specimens were stored in the refrigerator immediately after processing (Figure 2). Meanwhile, the oil sand powder generated from the processing was collected and used for subsequent X-ray diffraction tests.

2.2. Testing Equipment. This study included mineral composition tests, electron microscope scanning tests, grading analyses, and triaxial compression tests of the oil sand. A Dandong square circle DX-2500 diffractometer was used to test the mineral composition. SEM scanning and grading analysis were performed by field emission SEM, with a magnification of 25-800000 times and a minimum resolution of 1.0 nm. The triaxial compression experiment was completed with a MTS815 rock mechanics comprehensive experimental system with a maximum experimental temperature of 200°C, a temperature control accuracy of less than 0.5°C, a maximum axial load of 260 kN, an axial extensometer range of 15 mm, and a circumferential extensometer range of 10 mm.

Figure 1: Oil sand core at room temperature and in a frozen state.

Figure 2: Oil sand core test specimen preparation process by lathe and the processed test specimen.

2.3. Triaxial Compression Experimental Scheme at Different Temperatures and Confining Pressures. To restore the oil sand specimen as close as possible to its *in situ* state, first, a preconsolidation drainage experiment was carried out on the oil sand specimens, that is, the specimens were thawed in a triaxial chamber for 6 h under conditions of 500 kPa. When the water and heavy oil in the oil sand were fully thawed and easily flowed, the hydrostatic pressure was applied according to the stress path shown in Figure 3; in this case, the oil sand did not produce consolidation water pressure in the preconsolidation drainage experiment. The duration of the consolidation drainage process was 1.5 h, and the compression at the end of consolidation was the effective confining pressure C_p under triaxial loading. Then, heating was performed by an electric heating wire to heat the rock specimen to the design temperature (no heating was required for the experiment at room temperature). To avoid thermal rupture, the heating rate was 6°C/h, and the effective compression was constant during heating. According to the monitoring data, the temperature of high-pressure water vapor in the reservoir is generally between 70°C and 125°C; this study performed triaxial compression experiments at room temperature (RT), 75°C, and 120°C. Finally, an axial load was applied under an effective confining pressure with circumferential displacement control. The loading rate was 0.03 mm/min. The experiment was stopped when the axial strain reached 9%. According to the field stress test of the Fengcheng oil sand reservoir, triaxial compression experiments were performed at room temperature with effective confining pressures of 0.5 MPa, 1 MPa, 2 MPa, and 5 MPa.

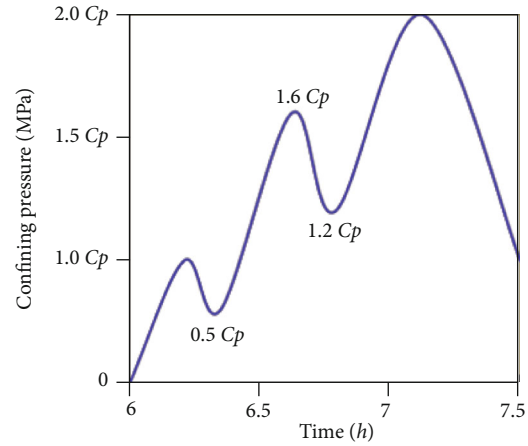

Figure 3: Schematic of the preconsolidation loading of the oil sand specimens (C_p is the effective confining pressure during the triaxial test).

When the effective confining pressure was 0.5 MPa and 5 MPa, high-temperature triaxial confining pressure experiments were also carried out at 75°C and 120°C. A summary of the specimen numbering scheme and experimental boundary conditions is shown in Table 1.

3. Experimental Results and Discussion

3.1. Characteristics of the Mineral Composition and Cementation State of Oil Sand. The main mineral types and contents of the oil sand tested by X-ray diffraction are summarized in Table 2. The main minerals in the oil sand were quartz, albite, and potassium feldspar. The clay mineral content was lower than the quartz, albite, and potassium feldspar contents. Although all the oil sand specimens were taken from the same reservoir, the mineral contents vary greatly among the specimens. The quartz content was 33%~59%, with an average of 43.75%. The sodium feldspar content was 24%~46%, with an average of 35.25%. The potassium feldspar content was 9%~21%, with an average of 14.00%. The content of clay minerals was 3%~11%, with an average value of 7.25%. Compared to Canadian Cold Lake oil sand [27], Fengcheng oil sand has more quartz and feldspar, which is the main reason for the great difference between the characteristics of these two types of oil sand [22].

Figure 4 shows three typical SEM images of Fengcheng oil sand. The quartz and feldspar particles in the oil sand were loose, and the bond between particles was weak. Some of the mineral particles in the oil sand were larger, resulting in pores that had no filling materials and a larger porosity, which provided effective flow passages for high-viscosity heavy oil exploitation [28]. Some oil sand specimens had a high content of heavy oil (the pores between the mineral particles were filled with heavy oil (asphalt)), and some oil sand pores were filled with soft clay minerals. Because the strength of clay minerals is low and the clay mineral content is generally less than 10%, the cohesion of the oil sand should be low, but both quartz and feldspar particles are rough and may interlock, which is helpful to enhance the oil sand strength.

Table 1: Numbering of the oil sand specimens and their corresponding experimental conditions.

Rock type	Specimen	Experimental temperature	Effective confining pressure (MPa)
Oil sand	L1	Room temperature (RT)	0.5
	L2	Room temperature (RT)	1
	L3	Room temperature (RT)	2
	L4	Room temperature (RT)	5
	L5	75°C	0.5
	L6	75°C	5
	L7	120°C	0.5
	L8	120°C	5

Table 2: Primary mineral contents in the oil sand (%).

Specimen	Quartz	Albite	Clay	Feldspar
L1	35	36	11	18
L2	49	31	11	9
L3	59	24	3	14
L4	49	32	6	13
L5	33	43	4	21
L6	36	42	6	16
L7	36	46	8	11
L8	53	28	9	10
Average values	43.75	35.25	7.25	14

3.2. Characteristics of the Particle Size Distribution of Oil Sand. The particle size distribution of oil sand has an important effect on its physical and mechanical properties. Figure 5 shows three typical statistical characteristics of oil sand particle size. The particle sizes of the first type of oil sand were 125~475 μm: the mineral particle size was mainly concentrated in the range of 200~350 μm, and the other particle sizes were smaller. The particle sizes of the second type of oil sand were 75~300 μm, and the maximum mineral particle size was 135~150 μm. As the size interval increases, the total number of particles first increased and then decreased. The particle sizes of the third type of oil sand were 120~420 μm. Within the particle size range of 13~210 μm, the number of particles in each particle size interval varied little. Most of the particles were concentrated within 240~270 μm, and there were few particles larger than 360 μm. The particle sizes of these Fengcheng oil sands are similar to those of fine sand and medium sand [29], and the average particle size of these Fengcheng oil sands is less than that of the Kuwaiti oil-bearing sand mixture [30]. The grain size distribution histogram of the Fengcheng oil sand was analyzed by normal distribution, logarithmic distribution, Weibull distribution, Poisson distribution, and other probability distribution functions. Only the logarithmic distribution function has a good fitting degree for oil sand specimen 2 (Figure 5(b)); the commonly used probability distribution functions cannot fit the particle size distributions of oil sand specimens 1 and 3 well (Figures 5(a) and 5(c)).

Analogizing the accumulation curves of the oil sand with different particle gradations of soil [27], Figure 6 shows the cumulative percentage of oil sand mineral particles with particle size. According to the statistical analysis, it was found that for specimen 1, D_{10} (representing 10% of the total particle size, D_{60} and D_{30} are similarly defined below) was 188 μm, D_{30} was 220 μm, and D_{60} was 278 μm. For specimen 2, D_{10} was 114 μm, D_{30} was 142 μm, and D_{60} was 175μm. For specimen 3, D_{10} was 168 μm, D_{30} was 218 μm, and D_{60} was 255 μm. In general, we can assume that D_{10} squared was positively correlated with the permeability of oil sand [31, 32], indicating that the permeabilities of specimen 1 and specimen 3 were better than the permeability of specimen 2, which is consistent with the SEM scanning results shown in Figure 4. The value of D_{60} was near the median value of the specimen particle size distribution, indicating that the particle size distribution of oil sand has good continuity. On the basis of the characteristic parameters of the cumulative particle size distribution of oil sand above, the nonuniformity coefficient C_u and curvature coefficient C_c of oil sand can be obtained according to the following formula [33]:

$$C_u = \frac{D_{60}}{D_{10}},$$
$$C_c = \frac{D_{30}^2}{(D_{60} \times D_{10})}. \quad (1)$$

The calculated nonuniformity coefficients of the three specimens were 1.48, 1.54, and 1.52, respectively, and the calculated curvature coefficients were 0.93, 1.01, and 1.11, respectively. The nonuniformity coefficients of the oil sand were small, which indicated that the corresponding gradations were good and easier to compact. However, this makes the porosity of oil sand easier to reduce under external forcing and thermal loading, which is not conducive to reservoir stimulation because it reduces the effective permeability of the reservoir for oil sand exploitation and increases the difficulty of the efficient exploitation of oil sand.

3.3. Characteristics of Oil Sand Stress-Strain Curves under Different Confining Pressures and Temperatures. The deformation characteristics of oil sand under different external conditions are an important basis for judging the effect of steam-assisted gravity drainage technology on reservoir stimulation. Figure 7 shows the deviatoric stress-axial strain curve and volumetric strain-axial strain curve of oil sand under different temperatures and confining pressures. When the initial preconsolidation stress (Figure 3) was small, during the initial stage of applying the axial stress, the deviatoric stress-axial strain curve was concave; however, when the preconsolidation stress was large, the deviatoric stress-axial strain curve changed linearly. On the whole, the prepeak deformation characteristics of oil sand under different temperatures and confining pressures were similar. With the increase in axial stress, plastic deformation clearly occurred after the elastic deformation, and the prepeak plastic deformation and circumferential deformation decreased with the increase in confining

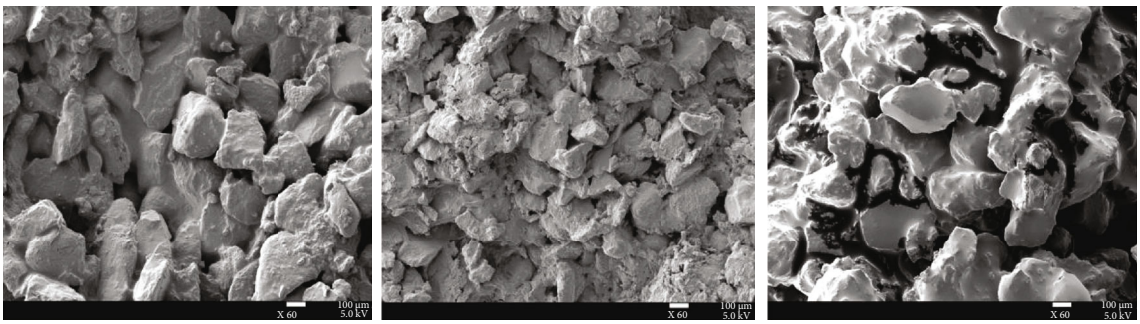

Figure 4: SEM images of oil sand.

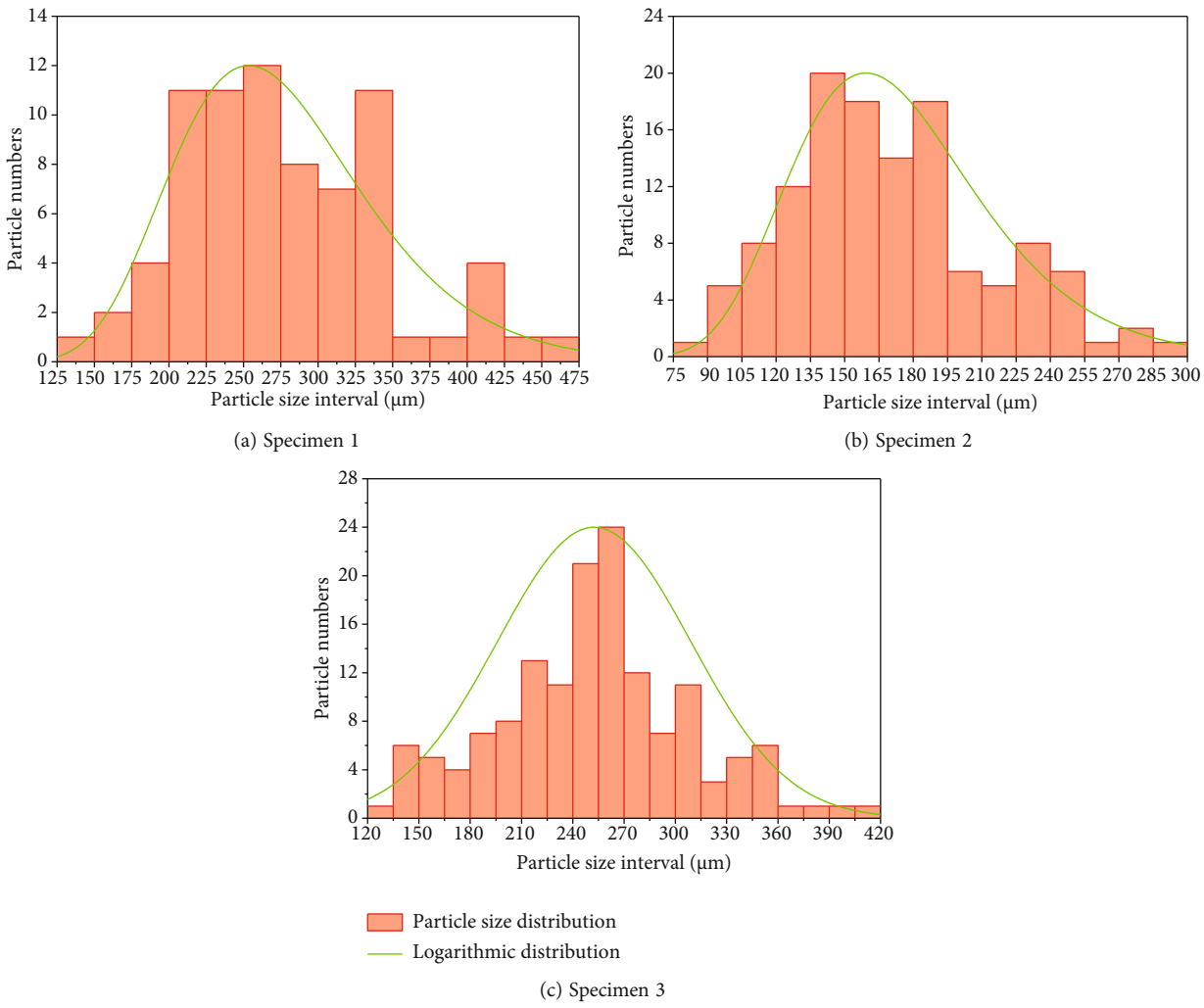

Figure 5: Particle size distribution and optimal probability distribution of the mineral particles in three oil sand specimens.

pressure. However, there were obvious differences in the postpeak deformation of the oil sand under different temperatures and confining pressures.

At room temperature, the confining pressure was 0.5 MPa, and the deviatoric stress of the oil sand decreased very little after peaking. Thus, it can be considered that the deformation of the studied oil sand enters the state of complete plastic flow, which is similar to that of Cold Lake oil sand under low stresses [16]. With the increase in deviatoric stress and axial strain, the volumetric strain of the Fengcheng oil sand remained constant. In this state, even if an external load was applied, the oil sand permeability may not have changed with strain, which was not conducive to reservoir transformation. Under confining pressures of 1 MPa, 2 MPa, and 5 MPa, the postpeak deformation was strain softening. Notably, although the heat shrink film used in the triaxial experiment has a certain deformation ability, when the axial deformation of the specimen was large

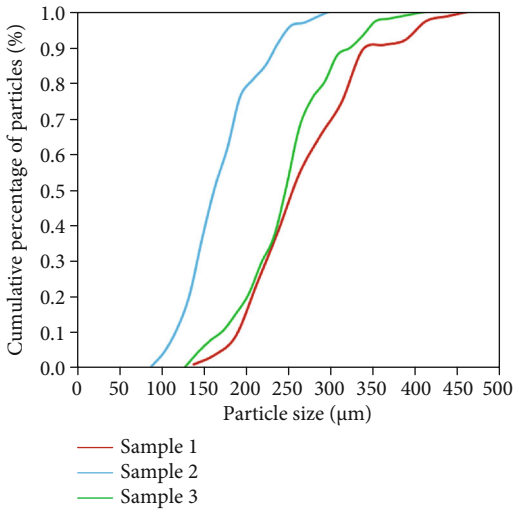

Figure 6: Cumulative distribution curves of the mineral particles in the oil sand specimens.

enough, the heat shrink film restricts the circumferential deformation of the specimen, which caused the rise at the end of the volumetric strain-axial strain curve for most oil sand specimens.

The increase in temperature made the oil sand deformation more complicated. When the confining pressure was 0.5 MPa, under the conditions of temperatures of 75°C and 120°C, with the increase in axial deformation, the postpeak stress first decreased and then increased, that is, strain softening occurred before strain hardening. When the confining pressure was 5 MPa and the temperature was 75°C, the deformation showed the same characteristics as above. When the confining pressure was 5 MPa and the temperature was 120°C and with the increase in axial strain, the oil sand shows the characteristics of first strain softening and then strain hardening and finally strain weakening. There may be two reasons for the postpeak deformation of oil sand under the above high-temperature conditions: one is the complex relative motion of the mineral particles in the oil sand, resulting in self-locking under the action of temperature and stress, and the other is the local compression after the peak, causing the oil sand porosity to decrease and the oil sand strength to increase [34].

The permeability of oil sand reservoirs is closely related to the volume expansion of the oil sand; therefore, according to the volumetric strain-axial strain curve, the shear dilatation rate is defined as the ratio of the volumetric strain change and the axial strain change values in the oil sand volume expansion stage. The shear dilatation rate of oil sand at different temperatures and confining pressures is shown in Figure 8. Due to the inhomogeneity of the specimen itself, the strength of specimen L4 (with a confining pressure of 5 MPa at room temperature) was significantly lower than the result of other specimens, so the experimental results of L4 were not taken into account when discussing the shear dilatation rate. The shear dilatation rate of oil sand clearly decreased with increasing confining pressure. At room temperature, when the confining pressure increased from 0.5 MPa to 2 MPa, the shear dilatation rate decreased 4.7 times. The relationship between the confining pressure and shear dilatation rate was significantly nonlinear, similar to those of Cold Lake oil sand and Athabasca oil sand, but under similar confining pressures, the shear dilatation rates of Cold Lake oil sand were greater than those of the Fengcheng oil sand, and those of the Athabasca oil sand were less than those of the Fengcheng oil sand [16, 17].

The shear dilatation rate was greatly affected by temperature, and the shear dilatation rate at 75°C was higher than that at 120°C. When the confining pressure was 0.5 MPa, the shear dilatation rate at 75°C and 120°C was 1.6 times and 1.3 times that at room temperature, so the effect of temperature on the shear dilatation rate was much smaller than the effect of confining pressure. The most suitable injection pressure and temperature can be used to maximize the shear dilatation rate of the reservoir.

3.4. Variation Characteristics of the Mechanical Parameters of Oil Sand under Different Confining Pressures and Temperatures. The mechanical parameters of oil sand are the key factors in the design of oil sand exploitation schemes. Figure 9 summarizes the compressive strength of oil sand at different confining pressures and temperatures. At room temperature (RT), the compressive strength of the oil sand increased linearly with the confining pressure (the experimental results of L4 specimens clearly include error due to their heterogeneity, so the experimental results of L4 are not discussed in this section). When the confining pressure increased from 0.5 MPa to 2 MPa, the compressive strength of the oil sand increased 3 times. As the temperature increased, the strength of the oil sand did not weaken, and the triaxial compression of the Athabasca oil sand also indicated that temperature has little influence on the peak strength [13]. When the confining pressure was 0.5 MPa, the compressive strengths of the oil sand at 75°C were higher than those at 120°C, and when the confining pressure was 5 MPa, the variation in the compressive strength at these two temperatures was opposite to that at 0.5 MPa.

Figure 10 shows the variation characteristics of the residual strength of oil sand at different confining pressures and temperatures. At room temperature, there was a linear relationship between the residual strength and confining pressure, which was the same as that of the compressive strength and confining pressure. When the confining pressure remained the same, the residual strength under different temperature experimental conditions nearly remained the same. Thus, it can be considered that temperature has no effect on the residual strength of oil sand; this finding is different from the phenomenon suggesting that the residual strength of Athabasca oil sand is greatly affected by temperature [13]. The ratio of compressive strength to residual strength of oil sand can be calculated from Figures 9 and 10, as shown by the data points marked with solid shapes in Figure 10. The ratio of peak strength to residual strength under other experimental conditions was between 1.1 and 1.25 except for the high-temperature experiment with a

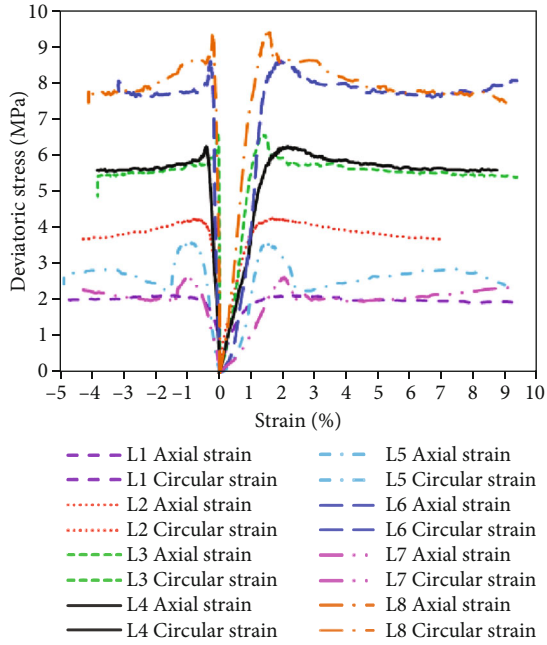

(a) Deviatoric stress–axial strain curves and deviatoric stress–circumferential strain curves of the oil sand

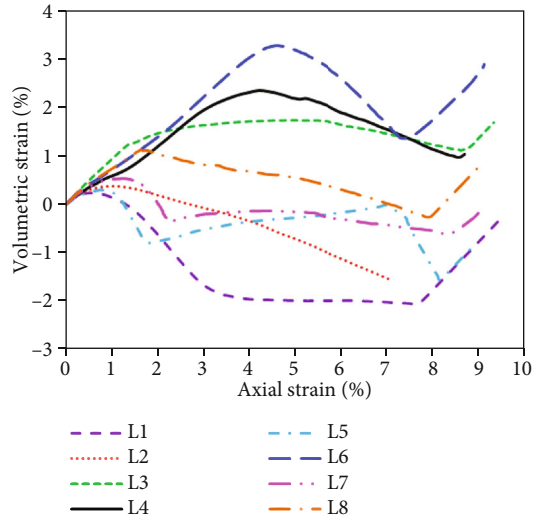

(b) Deviatoric stress–volumetric strain curves of the oil sand

Figure 7: Characteristics of oil sand deformation under different temperatures and confining pressures.

confining pressure of 0.5 MPa, which further indicated that the strain softening characteristics of oil sand were relatively weak.

The variations in the elastic modulus and Poisson's ratio of oil sand under different confining pressures and temperatures are shown in Figures 11 and 12, respectively. The confining pressure has a significant effect on the elastic modulus and Poisson's ratio of oil sand. At room temperature, the elastic modulus increased linearly with increasing confining pressure, while Poisson's nonlinearly decreased. When the confining pressure increased 4 times, the elastic modulus increased 3.5 times and Poisson's ratio decreased 1.3 times, indicating that the fine mineral particles of the oil sand loosened and that the specimen compacted effectively through the preconsolidation process. At a low confining pressure, the elastic moduli of the oil sand at 75°C were significantly higher than those at room temperature and 120°C. At a high confining pressure, the elastic moduli peaked at 120°C. The effect of high temperatures on the elastic modulus of oil sand was not clear, so it was necessary to carry out in-depth analysis of oil sand experiments under various temperature gradients. When the confining pressure was 0.5 MPa, Poisson's ratio of the oil sand could be influenced significantly; with the increase in confining pressure, the effect of temperature on Poisson's ratio decreased; when the confining pressure was 5 MPa, Poisson's ratio changed very little under the different temperature conditions studied. In summary, the influence of confining pressure on the elastic modulus and

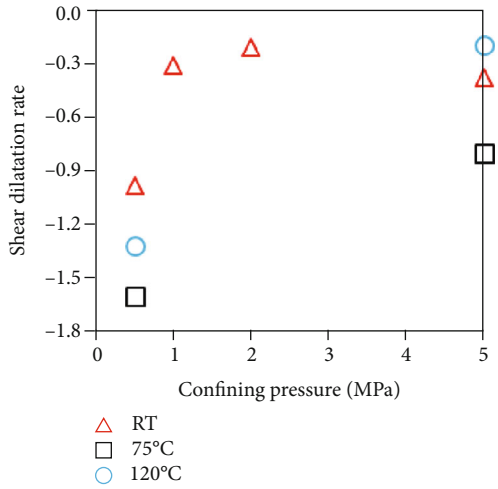

Figure 8: Characteristics of the oil sand shear dilatation rate under different confining pressures and temperatures.

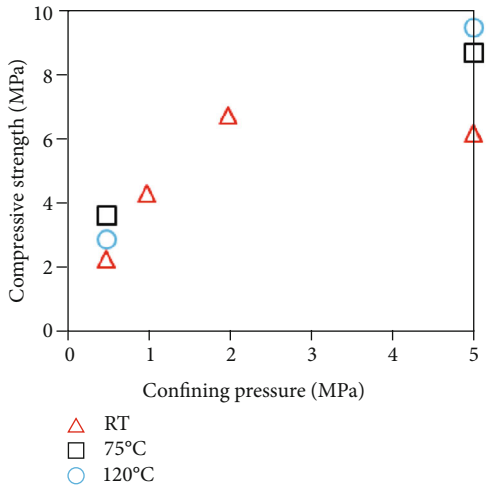

Figure 9: Characteristics of oil sand compressive strength under different confining pressures and temperatures.

Poisson's ratio of oil sand was greater than the influence of temperature [13, 14]. Compared with the elastic modulus and Poisson's ratio of Cold Lake oil sand and Athabasca oil sand, the elastic modulus of Fengcheng Oilfield was similar to that of oil sand under similar confining pressure, which is much smaller than that of Athabasca oil sand.

3.5. Characteristics of the Oil Sand Failure Mode. The failure path of oil sand will provide an effective channel for heavy oil exploitation. Figure 13 shows the failure mode of the oil sand at different confining pressures and temperatures. At room temperature, when the confining pressures were 0.5 MPa and 1 MPa (L1 and L2), the macrocracks generated were parallel to the loading direction due to the transverse tensile stress generated by axial loading. In this case, the overall deformation of the oil sand specimens was uniform. When the confining pressures were 2 MPa and 5 MPa (L3 and L4), the oil sand specimens clearly formed multiple

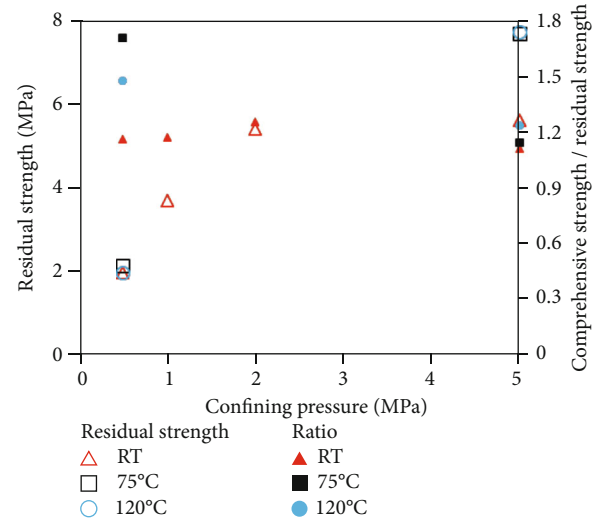

Figure 10: Characteristics of oil sand residual strength under different confining pressures and temperatures (the hollow and solid shapes represent the residual strength and ratio of compressive strength to residual strength, respectively).

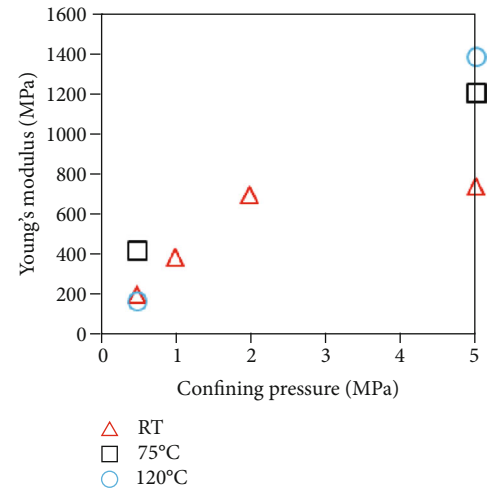

Figure 11: Characteristics of oil sand Young's modulus under different confining pressures and temperatures.

near-parallel shear cracks, which was conducive to improving the overall permeability coefficient of the specimens. The postpeak volume deformation was mainly caused by the slippage along the shear planes of the specimens under axial loading, which is similar to the failure model of Athabasca oil sand under different confining pressures [15].

When the experimental temperature was 75°C (L5 and L7) and the confining pressure was 0.5 MPa and 5 MPa, the oil sand specimens formed conjugate shear surfaces, which was different from the failure mode of the oil sand specimens observed at room temperature and under the same confining pressure. During the high temperature, the stiffness of heat shrinkage film is large. It would impose restrictions on the specimen deformation; therefore, the stress after peak load of specimen L5 is becoming higher

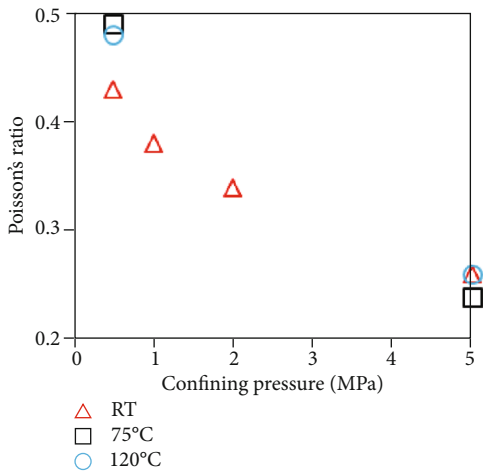

Figure 12: Characteristics of oil sand Poisson's ratio under different confining pressures and temperatures.

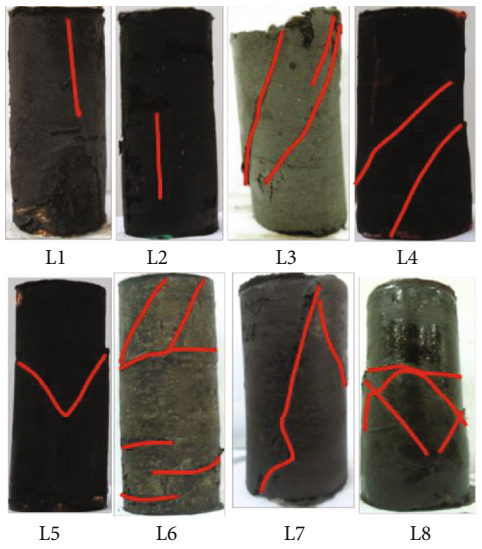

Figure 13: Failure patterns of oil sand under different confining pressures and temperatures.

with the increment of strain. When the experimental temperature was 120°C (L6 and L8), the oil sand specimens under different confining pressures exhibited not only multiple shear surfaces but also transverse macroscopic cracks in the vertical axial loading direction, possibly due to the tensile stress induced under high-temperature conditions, making the failure mode of the oil sand at this temperature more complex. If the confining pressure and temperature were properly increased, more macroscopic cracks would be generated in the oil sand, which could provide more flow channels for heavy oil exploitation.

4. Conclusion

Using Xinjiang Fengcheng Oilfield oil sand reservoir core from depths greater than 400 meters, this work studied the mineral composition and particle size distribution of the oil sand to obtain its mesoscopic structure characteristics, and oil sand specimens were tested under four different confining pressure and three temperature conditions via conventional triaxial compression tests. The mesoscopic structure, deformation, mechanical parameter changes, and failure modes of the oil sand were analyzed in detail considering the different confining pressures and temperatures. The main conclusions of this study are as follows:

(1) The minerals in the oil sand were mainly quartz, feldspar, and clay minerals, of which the total content of quartz and feldspar was generally more than 90%. The mesostructure of the mineral particles in the Fengcheng oil sand was loose, and the pores between minerals were mainly filled by heavy oil or clay minerals with a low cohesive force

(2) The grain size distributions of the oil sand minerals were similar to those of fine sand and medium sand. The common normal distribution and Weibull distribution could not fit the change in oil sand particle quantity with particle size. The nonuniformity coefficient of the oil sand mineral particles was small, the gradation was good, and the particles were easily compacted, which was not conducive to the oil sand reservoir properties

(3) Under different temperatures and confining pressures, the prepeak plastic deformation of oil sand exhibited obvious plastic deformation after elastic deformation, and the prepeak plastic deformation and circumferential deformation decreased with increasing confining pressure, which was very different. The shear dilatation rate of the oil sand decreased nonlinearly with increasing confining pressure, and increasing the temperature helped to improve the shear dilatation rate of the oil sand

(4) The compressive strength, residual strength, and elastic modulus of the oil sand increased linearly with increasing confining pressure, while Poisson's ratio decreased nonlinearly with increasing confining pressure. The effect of temperature on the strength and modulus of elasticity of the oil sand was small, but temperature could significantly affect Poisson's ratio of the studied oil sand

(5) In the experiments at room temperature and 75°C, the main macroscopic cracks observed in the oil sand specimens were vertical, and shear cracks were produced by transverse tensile stress; in the experiment at 120°C, the thermal stress induced by the high temperature caused transverse cracks to form in the oil sand specimens. Properly increasing the confining pressure and temperature can produce more cracks and provide more flow channels for oil sand exploitation

Data Availability

All data generated or analyzed during this study are included in this published article.

Conflicts of Interest

The authors declare that there is no conflict of interest regarding the publication of this article.

Authors' Contributions

Liu Yang and Yufei Jiang contributed to the writing of the manuscript. Chao Gao revised the manuscript. All authors have read and agreed to the published version of the manuscript.

References

[1] A. Klerk, *Unconventional Oil: Oilsands, in "Future Energy"*, Elsevier, 2020.

[2] Z. Shen, Z. Cao, X. Zhu, and X. Li, "Visbreaking of Chinese oil sand bitumen," *Petroleum Science and Technology*, vol. 26, no. 14, pp. 1676–1683, 2008.

[3] J. Liggio, S.-M. Li, K. Hayden et al., "Oil sands operations as a large source of secondary organic aerosols," *Nature*, vol. 534, no. 7605, pp. 91–94, 2016.

[4] A. Heyes, A. Leach, and C. F. Mason, "The economics of Canadian oil sands," *Review of Environmental Economics and Policy*, vol. 12, no. 2, pp. 242–263, 2018.

[5] W. Montgomery, M. A. Sephton, J. S. Watson, H. Zeng, and A. C. Rees, "Minimising hydrogen sulphide generation during steam assisted production of heavy oil," *Scientific Reports*, vol. 5, no. 1, p. 8159, 2015.

[6] D. Z. Zhao, W. W. Sun, and M. Z. Sun, "The separating of inner Mongolian oil sand with ultrasound," *Petroleum Science and Technology*, vol. 29, no. 24, pp. 2530–2535, 2011.

[7] X. Dong, H. Liu, Z. Chen, K. Wu, N. Lu, and Q. Zhang, "Enhanced oil recovery techniques for heavy oil and oilsands reservoirs after steam injection," *Applied Energy*, vol. 239, pp. 1190–1211, 2019.

[8] X. He, L. Zhang, Y. Huang, H. Yang, and S. Chen, "Study on evaluation method of capacity expansion effect of Fengcheng SAGD oil sand microfracturing," *Xinjiang Oil and Gas*, vol. 13, no. 3, pp. 29–32, 2017.

[9] Y. Gao, M. Chen, B. Lin, Y. Jin, and H. Pang, "Study on compressibility during micro-fracturing in continental ultra-heavy oil sand reservoirs-taking the Qigu formation of Xinjiang Fengcheng oilfield Z1 block for instance," *Petroleum Science Bulletin*, vol. 2, no. 2, pp. 240–250, 2017.

[10] Y. Gao and M. Chen, "Numerical modeling on thermoelastoplastic responses of Karamay oil sand reservoir upon steam circulation considering phase change of bitumen," *Journal of Petroleum Science and Engineering*, vol. 187, article 106745, 2020.

[11] Z. Wu, Y. Wu, S. Xu, J. Guo, L. Zhai, and X. Che, "Characteristics and evaluation of extremely shallow oil sand in a heavy oil reservoir," *Petroleum Science and Technology*, vol. 33, no. 11, pp. 1215–1221, 2015.

[12] Y. Wu, S. Xu, Z. Wu, Z. Wang, L. Zhai, and J. Wu, "Heating oil sand and effects on the interlayers," *Petroleum Science and Technology*, vol. 35, no. 1, pp. 9–15, 2017.

[13] S. C. Horner, S. M. Hubbard, H. K. Martin, C. A. Hagstrom, and D. A. Leckie, "The impact of Aptian glacio-eustasy on the stratigraphic architecture of the Athabasca Oil Sands, Alberta, Canada," *Sedimentology*, vol. 66, no. 5, pp. 1600–1642, 2019.

[14] M. B. Dusseault and N. R. Morgenstern, "Shear strength of Athabasca oil sands," *Canadian Geotechnical Journal*, vol. 15, no. 2, pp. 216–238, 1978.

[15] S. A. Aiban, "The effect of temperature on the engineering properties of oil-contaminated sands," *Environment International*, vol. 24, no. 1-2, pp. 153–161, 1998.

[16] R. Wong, W. E. Barr, and P. R. Kry, "Stress–strain response of Cold Lake oil sands," *Canadian Geotechnical Journal*, vol. 30, no. 2, pp. 220–235, 1993.

[17] A. M. Samieh and R. C. K. Wong, "Deformation of Athabasca oil sand at low effective stresses under varying boundary conditions," *Canadian Geotechnical Journal*, vol. 34, no. 6, pp. 985–990, 1997.

[18] D. S. Ardeshir and G. J. Tim, "Oil sand deformation under cyclic loading of ultra-class mobile mining equipment," *Journal of Terramechanics*, vol. 47, no. 2, pp. 75–85, 2010.

[19] Z. Wang and R. C. Wong, "Strain-dependent creep behavior of Athabasca oil sand in triaxial compression," *International Journal of Geomechanics*, vol. 17, no. 1, p. 04016027, 2017.

[20] Z. Wang, R. Wong, and L. Qiao, "Research on creep characteristics and constitutive model of oil sand," *Chinese Journal of Geotechinical Engineering*, vol. 34, no. 8, pp. 1412–1424, 2012.

[21] L. Qiao, J. Dai, Z. Wang, and B. Xu, "Experimental study on mesostructure and mechanical properties of Fengcheng oil sand," *China Civil Engineering Journal*, vol. 48, no. s2, pp. 59–63, 2015.

[22] C. Li, L. Xie, S. Chen, S. Dou, and B. Xu, "Experimental research on mechanical and thermal properties of oil sand," *Rock and Soil Mechanics*, vol. 36, no. 8, pp. 2298–2306, 2015.

[23] J. Wang, L. Xie, H. Xie, and C. Li, "Triaxial mechanical characteristics and constitutive model of oil sand in Fengcheng," *Journal of Sichuan University*, vol. 47, no. 5, pp. 1–9, 2015.

[24] Y. Gao, M. Chen, B. Lin, Y. Jin, S. Chen, and H. Yu, "Thermal influences on mechanical properties of oil sands," *Chinese Journal of Rock Mechanics and Engineering*, vol. 37, no. 11, pp. 402–402, 2018.

[25] B. Lin, Y. Jin, H. Pang, and A. B. Cerato, "Experimental investigation on dilation mechanisms of land-facies Karamay oil sand reservoirs under water injection," *Rock Mechanics and Rock Engineering*, vol. 49, no. 4, pp. 1425–1439, 2016.

[26] H. Pang, Y. Jin, and Y. Gao, "Evaluation of elastic property changes in Karamay oil sand reservoir during thermal stimulation," *Energy Science & Engineering*, vol. 7, no. 4, pp. 1233–1253, 2019.

[27] S. He, F. J. Longstaffe, and Z. Zhou, "Stable isotopes of clay minerals from autoclave tests of oil sands: implications for clay formation during steaming of Alberta Clearwater oil sands," *Applied Geochemistry*, vol. 104, pp. 202–209, 2019.

[28] Z. A. Zhou, H. Li, R. Chow, O. B. Adeyinka, Z. Xu, and J. Masliyah, "Impact of fine solids on mined athabasca oil sands extraction II. Effect of fine solids with different surface wettability on bitumen recovery," *The Canadian Journal of Chemical Engineering*, vol. 95, no. 1, pp. 120–126, 2017.

[29] W. Powrie, *Soil Mechanics: Concepts and Applications*, CRC Press, 2018.

[30] H. A. Al-Sanad, W. K. Eid, and N. F. Ismael, "Geotechnical properties of oil-contaminated Kuwaiti sand," *Journal of Geotechnical Engineering*, vol. 121, no. 5, pp. 407–412, 1995.

[31] Y. Fujikura, "Estimation of permeability for sand and gravel based on pore-size distribution model," *Journal of Materials in Civil Engineering*, vol. 31, no. 12, p. 04019289, 2019.

[32] A. F. Elhakim, "Estimation of soil permeability," *Alexandria Engineering Journal*, vol. 55, no. 3, pp. 2631–2638, 2016.

[33] D. M. Carlos, J. R. Carneiro, M. Pinho-Lopes, and M. de Lurdes Lopes, "Effect of soil grain size distribution on the mechanical damage of nonwoven geotextiles under repeated loading," *International Journal of Geosynthetics and Ground Engineering*, vol. 1, no. 1, p. 9, 2015.

[34] T. Wong and P. Baud, "The brittle-ductile transition in porous rock: a review," *Journal of Structural Geology*, vol. 44, pp. 25–53, 2012.